

## Observation of structure changes for Li/Cu(111) by photoemission from Li core and quantum-well states

A. Carlsson, D. Claesson, G. Katrich,\* S.-Å. Lindgren, and L. Walldén  
*Physics Department, Chalmers University of Technology, 41296 Göteborg, Sweden*

(Received 28 October 1997)

Via photoemission from discrete quantum-well valence states and the Li  $1s$  core level, three different types of atom rearrangements are observed for Cu(111)/Li. In the monolayer coverage range gradual energy shifts for the core-level as well as a quantum-well state reflect a gradual lateral compression of the Li overlayer as more atoms are adsorbed. The onset of Li substitution and formation of a  $(2 \times 2)$  structure when, at RT, monolayer Li coverage is exceeded, is monitored via the disappearance and appearance of quantum-well states characteristic of the adsorbed full monolayer of Li and the part substitutional  $(2 \times 2)$  structure, respectively. A splitting of the Li  $1s$  emission peak into a doublet reflects the two different Li sites characteristic of the  $(2 \times 2)$  phase. A small energy shift of the quantum-well state (25 meV) indicates that, if it is cooled (170 K), the substitutional structure is unstable with respect to Li adsorption. [S0163-1829(98)01619-1]

### I. INTRODUCTION

In a thin metal film on a metal substrate valence electrons may be confined to the overlayer and form as discrete quantum-well-like states (DQWS's).<sup>1</sup> This can happen if the substrate has a band gap since, within the gap, states may extend only with an oscillating tail on the substrate side of the metal/metal interface. Even for energies outside band gaps the interface reflectivity may be sufficient to give resonant quantum-well-like states with a modest energy spread.<sup>2,3</sup> If DQWS's are found at energies near the Fermi level, photoemission lines are narrow for a well-ordered sample due to the long hole lifetime, and the temperature-dependent width of the Lorentzian line obtained is given by the electron-phonon scattering rate.<sup>4-6</sup> Narrow lines are obviously advantageous for observing small changes of energy and linewidth associated with a reordering of all or some of the atoms supporting a DQWS. In the present work DQWS's are observed near the Fermi energy for Cu(111)/Li. Via these states we observe four different types of atom rearrangements for the system, namely, (a) a gradual lateral compression of the monolayer (ML) as more Li atoms are accommodated, (b) the structure change reported recently by low-energy electron diffraction<sup>7</sup> (LEED) to a part substitutional  $(2 \times 2)$  structure obtained when the sample is held at RT and full monolayer coverage is exceeded, (c) a reordering of the  $(2 \times 2)$  structure upon deposition on a cooled sample of even small amounts of Li, and (d) an increase of the mean area for monolayer high islands of Li atoms on top of the first full Li layer as the second layer coverage increases.

A difference in character between (b) and (c) is that it takes a long time (half an hour) for the substitutional phase to form while no time delay is observed for (c), which means that it is complete in less than 1 min after a Li deposit. Observations (a)–(d) are all revealed via energy shifts or characteristic energies of DQWS's near the Fermi level. The structure changes (a) and (b) are observed also via core-level photoemission. When monolayer coverage is exceeded such that the  $(2 \times 2)$  structure is formed, the Li  $1s$  peak is split

into a doublet indicating the existence of two different Li sites. Here we will consider mainly (b) and (c), but for the discussion of (b) we will use the results obtained for the monolayer state (a). Observations similar to (a) and (d) have previously been made for Na-covered Cu(111).<sup>5</sup>

### II. EXPERIMENT

The present photoemission spectra are angle resolved and recorded, using  $p$ -polarized light, along the surface normal of a Cu(111) crystal kept at RT or 170 K and covered with different amounts of Li. Three different experimental systems are used, two of which are connected to beam lines at the MAX Synchrotron Radiation Laboratory in Lund (Sweden). Of the spectra presented in this paper, those recorded using a photon energy of 6 eV are obtained at the uv beam line (BL 52) that is equipped with a normal incidence monochromator and the spectra recorded using 70- and 100-eV photons are measured at the toroidal-grating monochromator beam line (BL 41). The third system used is a high-resolution spectrometer (5 meV, Leybold Heraeus, EL22) with a 1-mW He-Cd laser ( $h\nu = 3.82$  eV) as a light source. As described in Ref. 5 the laser gives sufficient intensity to probe sparsely populated states in a small but often interesting range of energies above  $E_F$ .

The alkali metal is deposited at a rate of around 0.01 Å/sec in good UHV (low,  $10^{-10}$ -torr range) by heating a Li-filled Mo crucible, which is mounted inside water-cooled walls of a separate vacuum chamber connected to the main experimental chamber via straight-through valves such that the evaporation source may be mounted on either of the three spectrometers utilized. The source is kept at a constant temperature during an experimental run and the coverage is obtained from the evaporation time, using as a reference the time required to form one full atomic layer of Li. We assume that the saturation of the shift of a DQWS characteristic of the monolayer marks the completion of this layer.<sup>5</sup> The coverage values given below are thus based on the assumption that the sticking coefficient is independent of the Li coverage.

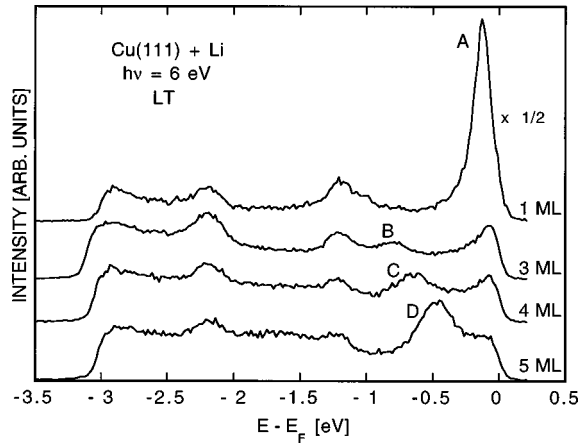


FIG. 1. Photoelectron-energy spectra recorded along the surface normal of Cu(111) held at 170 K and covered with 1, 3, 4, and 5 atomic layers of Li. The peaks A, B, C, and D are due to discrete quantum-well states while the peaks at  $-1.2$  and  $-2.2$  eV are due to the substrate.

No significant degradation of spectra is noted during a typical experimental run, which shows that contamination is not important for the results presented below. For more details regarding the uptake from the ambient during measurement we refer to a recent report on the contamination-induced changes of vibrational electron-energy-loss spectra recorded for Cu(111)/Li.<sup>8</sup>

### III. RESULTS

#### A. Li on cooled Cu(111)

Li evaporated onto a cooled (170 K) Cu(111) crystal grows layer by atomic layer in the thickness range studied ( $<5$  ML). This is demonstrated by the uv photoelectron energy spectra in Fig. 1. These spectra show emission peaks due to the Cu  $3d$  and  $s,p$  bands (at  $-2.2$  and  $-1.2$  eV, respectively) and peaks (labeled A–D) due to DQWS's with  $k_{\parallel}=0$ , formed at energies within the 5-eV-wide Cu band gap at the  $L$  symmetry point of the Brillouin zone. This gap extends 0.8 eV below the Fermi energy ( $E_F$ ).<sup>9</sup> The DQWS energies are as expected from estimates made for a Li film growing layer by layer. For this one may use the phase condition that the phase change is a multiple of  $2\pi$  for an electron making a return trip in the overlayer between the vacuum barrier and the overlayer/substrate interface.<sup>1,10,11</sup> Of interest for the discussion below and in particular for the state characteristic of the monolayer coverage range (peak A in Fig. 1) is that the energy shifts gradually with Li coverage until saturation is reached at  $E_F - 135$  meV (Fig. 2). The downshift, measured with the high-resolution spectrometer and shown in Fig. 2, is similar to that previously observed for Na adsorbed on Cu(111).<sup>5</sup>

#### B. Li on Cu(111) at RT

At RT no more than one full monolayer of Li may be adsorbed on Cu(111). If more Li is deposited, the hexagonal close-packed overlayer structure, indicated by the LEED pattern for 1 ML sketched in Fig. 3(a) is replaced by a  $(2 \times 2)$  structure [Fig. 3(b)] as was first observed by Mizuno

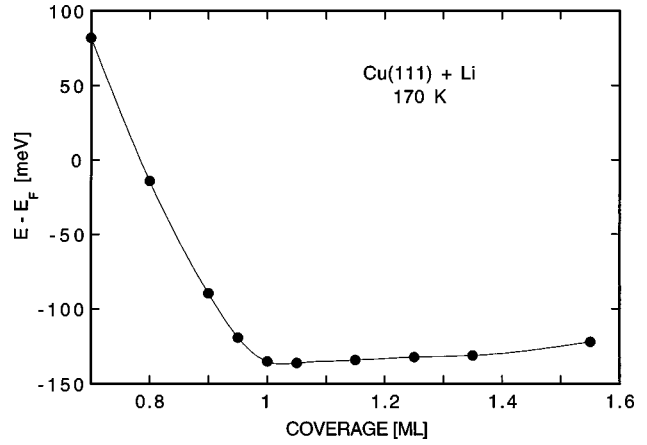


FIG. 2. Energy relative to the Fermi level vs Li coverage for a DQWS characteristic of Cu(111)/Li in the monolayer coverage range for a cooled sample (170 K).

*et al.*<sup>7</sup> From a dynamical LEED analysis they concluded that this structure is partly substitutional with  $\frac{1}{3}$  of the Li atoms replacing  $\frac{1}{4}$  of the Cu atoms in the uppermost substrate layer. On top of the mixed Cu/Li layer the remaining  $\frac{2}{3}$  of the Li atoms were found to form a honeycomb arrangement with each hexagonal cell centered above a substitutional site. The amount of Li required to form this  $(2 \times 2)$ -3Li structure corresponds to around 1.15 ML. The LEED pattern in Fig. 3(a) shows a weak doublet inside each of the six more intense spots due to the  $(10)$  beams from the substrate. This doublet is observed only for coverages close to a full monolayer and may, as for Li on Ru(0001),<sup>12</sup> be explained by a realignment of the incommensurate hexagonal overlayer structure away from the substrate orientation during the final compression of the monolayer. In our case this misalignment is  $4^\circ$  at a coverage of 1 ML.

#### 1. Core-level shifts

The sensitivity of core-level binding energies to the local surrounding makes photoemission from the Li  $1s$  state suitable to test if the configuration proposed for the observed  $(2 \times 2)$  pattern is plausible. In Fig. 4 are shown photoemission spectra, recorded at  $h\nu = 100$  eV, probing the Li  $1s$  core state at full monolayer coverage (1 ML) and at a coverage of 1.2 ML when the  $(2 \times 2)$  structure has formed. In the 1-ML

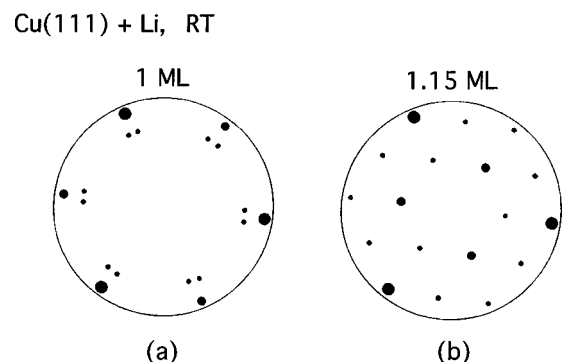


FIG. 3. Sketches of LEED patterns from Cu(111) held at RT and covered with 1 ML (a) and 1.15 ML (b) of Li. The electron energy is 68 eV.

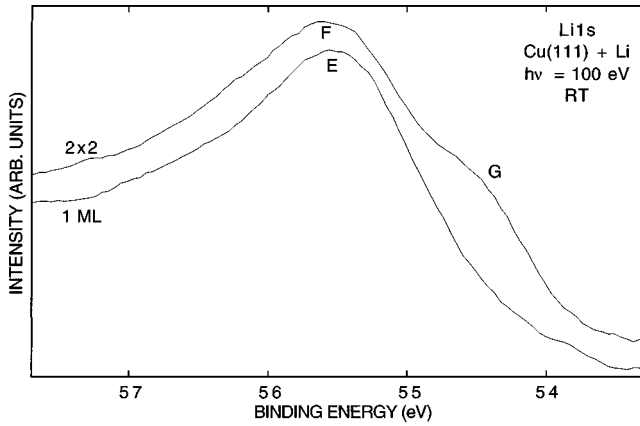


FIG. 4. Photoelectron energy spectra recorded in the Li 1s binding-energy range at  $h\nu = 100$  eV and along the surface normal of Cu(111) held at RT and covered with 1 ML and 1.2 ML of Li. For the labeling of peaks we refer to the text.

spectrum a single emission peak (*E*) is seen at a binding energy of 55.5 eV. As the  $(2 \times 2)$  structure forms, this peak splits into a doublet with a peak (*F*) at a slightly higher binding energy (0.05 eV) than that of *E* and a shoulder (*G*) on the low-binding-energy side. The shoulder is shifted downwards in binding energy by 1 eV relative to peak *E*.

In Fig. 5 are shown corresponding photoemission spectra for a number of submonolayer coverages. The Li 1s peak shifts to lower binding energy in a continuous manner as the coverage is increased without any abrupt changes in line-width or intensity. If the 1s binding energies are plotted versus coverage, one notes that the energy shift is small at coverages below 0.2 ML (Fig. 6). The total shift for the submonolayer coverage range probed (0.07–1 ML) is approximately 0.6 eV.

## 2. Valence states

For submonolayer coverages, the high-resolution photoemission results obtained at RT are similar to those obtained at 170 K with the difference that the DQWS at RT saturates at an initial-state energy of  $E_F - 110$  meV, which is 25 meV higher than for the cooled sample. Temperature cycling shows that the energy is not reversibly dependent on temperature. Upon cooling from RT to 170 K the energy remains nearly constant but if a full monolayer is deposited at 170 K and the sample then is allowed to reach RT, the initial energy shifts upwards by around 25 meV.

With standard resolution the main spectral changes induced by the adsorption-substitution structure change are that the energy distributions get wider by 0.3 eV and that the peak near  $E_F$  becomes strongly reduced (Fig. 7). The 0.3-eV work-function reduction is consistent with a reduced-Li coverage in the topmost layer. Between half- and full-monolayer coverage  $e\phi$  increases by approximately 0.6 eV (Ref. 8) and the value for the  $(2 \times 2)$  structure is obtained at 75% of the RT saturation coverage. While the presence of a small peak near the Fermi edge after the structure change might suggest that the structure change is incomplete, spectra recorded with high-energy resolution using the laser light source show that the weak peak near the Fermi edge is due to a weakly populated state 100 meV above  $E_F$  (peak *H* in Fig. 8). Further-

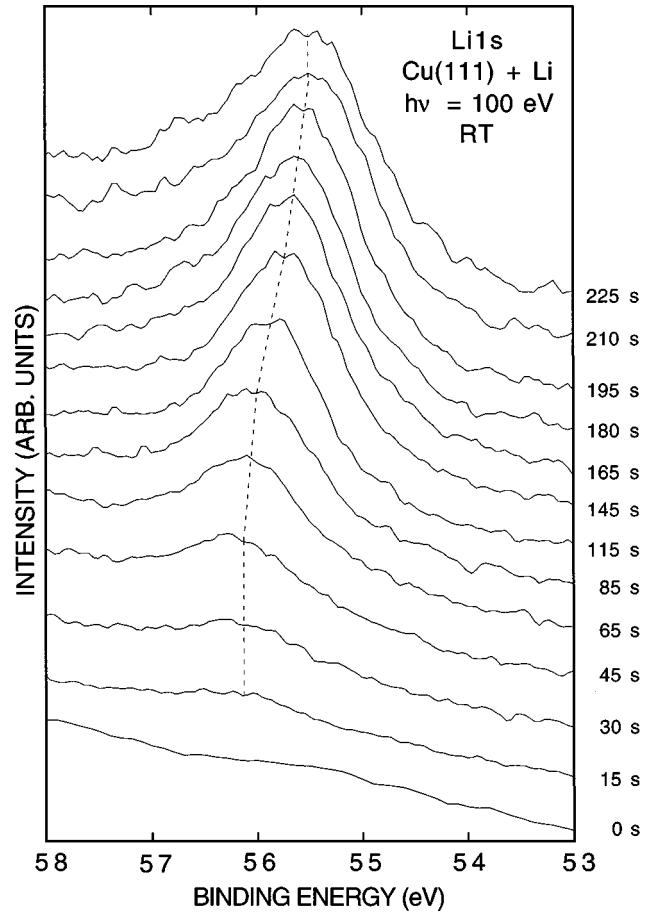


FIG. 5. Photoelectron-energy spectra from Cu(111) at RT recorded as those in Fig. 4 for a number of different submonolayer coverages of Li. The exposures are indicated by the evaporation times in seconds by the spectra, of which the uppermost one corresponds to deposition of a full monolayer.

more, the structure change is slow enough that it can be monitored via the replacement, with time, of the state 110 meV below  $E_F$  with the state 100 meV above  $E_F$ .

If, at RT, saturation coverage has been reached and another 15% of Li is deposited, the emission from the DQWS characteristic of 1 ML (see peak *A* in Fig. 8) decays gradually with time after the deposit and is replaced by emission

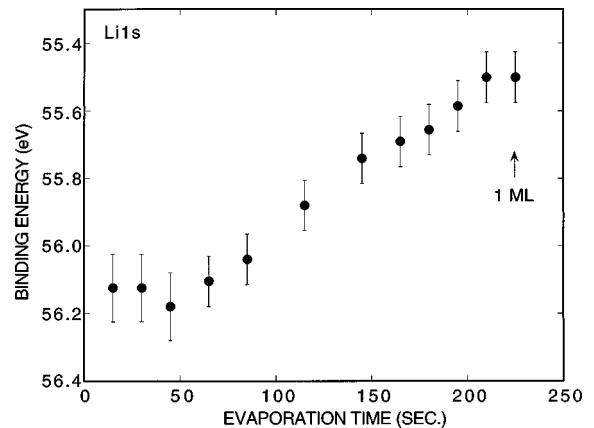


FIG. 6. Binding energy of the Li 1s state vs Li coverage on Cu(111) at RT obtained from the spectra in Fig. 5.

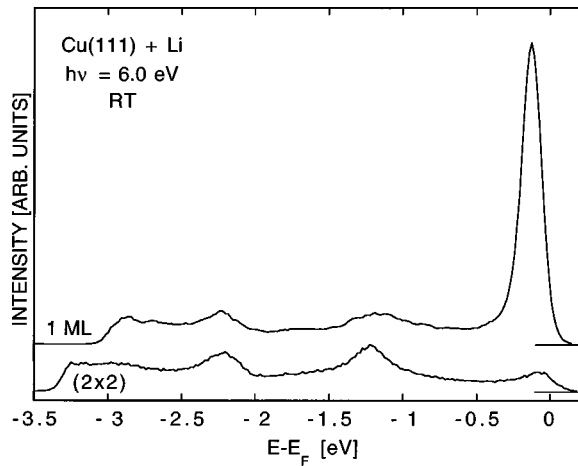


FIG. 7. Photoelectron energy spectra recorded at 6 eV photon energy along the surface normal for Cu(111) covered with a full monolayer of Li and for the part substitutional  $(2 \times 2)$  structure obtained when Li monolayer coverage is exceeded by 15%.

from a state at  $E_F + 100$  meV (peak *H* in Fig. 8). This peak is observed in raw spectra as a weak shoulder at the Fermi edge. To compensate for the reduced occupancy of states above  $E_F$ , the energy distributions in Fig. 8 are the recorded spectra multiplied by  $1 + \exp[(E - E_F)/kT]$ , i.e., the inverse of the Fermi-Dirac factor. We associate peak *H* with a DQWS characteristic of the  $(2 \times 2)$  structure.<sup>7</sup> Spectra recorded at higher photon energy reveal no additional DQWS's. Judged by the time dependence of the emission intensity from the 1-ML DQWS, the reordering is complete within around half an hour after the Li deposit (Fig. 9). The full drawn curve in Fig. 9 shows an exponential decay with a time constant of 8 min. The half hour required to complete the structure change is characteristic of the crystal used for the high-resolution

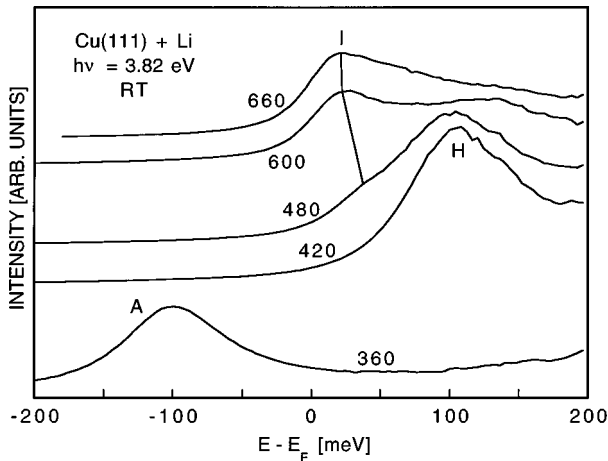


FIG. 8. Electron-energy spectra obtained after multiplication of photoelectron energy spectra by  $1 + \exp[(E - E_F)/kT]$  to compensate for the reduced occupancy for states near  $E_F$ . The sample is a Cu(111) crystal held at RT and covered with different amounts of Li indicated by the evaporation times given in seconds. Monolayer saturation coverage is obtained after 370 sec. The peaks labeled *A* and *H* are due to the discrete quantum-well states characteristic of the monolayer range and the  $2 \times 2$  structure, respectively. The spectrum with peak *H* is obtained half an hour after the 60-sec deposit made after recording the lower spectrum.

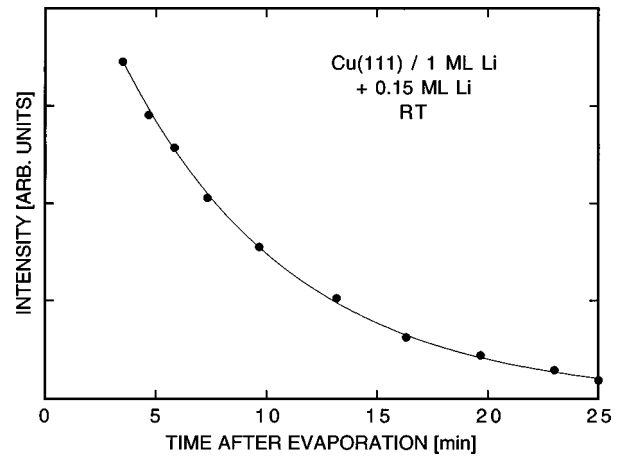


FIG. 9. Decay of the emission intensity due to the 1 ML DQWS plotted vs time after an increase of the Li deposit from 1 to 1.15 ML. The full drawn curve shows an exponential decay with 8-min time constant.

measurements. A different crystal was used in the synchrotron radiation laboratory and for this the structure change was complete in around 10 min. Both crystals have undergone the same treatment: electropolishing and Ar-ion bombardment ( $1 \mu\text{A}$ , 600 eV) followed by heating to around  $450^\circ\text{C}$ . Since also the vacuum conditions are similar, it would appear that the transformation time is sensitive to differences in surface quality that are small and out of our control.

In Fig. 10 are shown photoemission spectra recorded using 70-eV photons for (a) a clean Cu(111) surface, (b) full

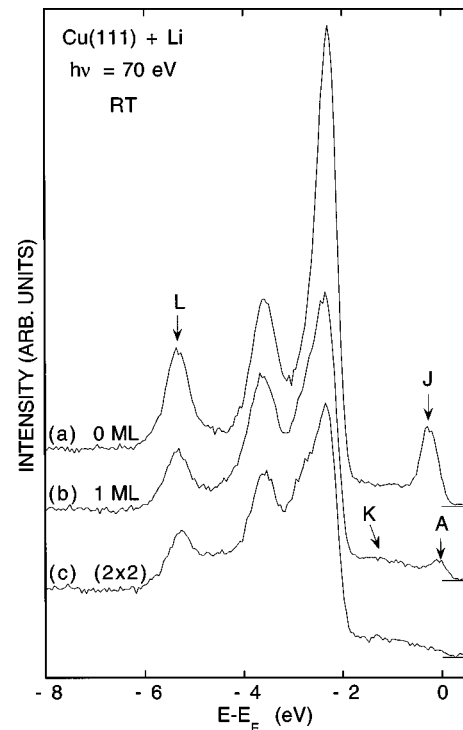


FIG. 10. Photoelectron energy spectra recorded at  $h\nu = 70$  eV along the surface normal of clean Cu(111) (a), Cu(111) covered with 1 ML of Li (b), and Cu(111) covered with 1.2 ML of Li (c). For the labeling of peaks we refer to the text.

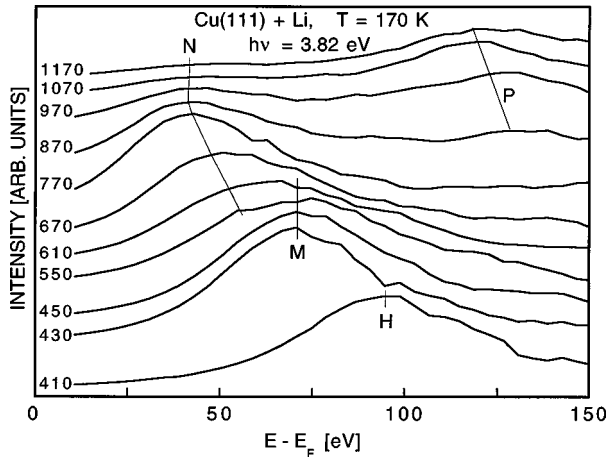


FIG. 11. Electron-energy spectra obtained as those shown in Fig. 8. The sample is Cu(111)/Li, which after transformation at RT to the substitutional structure is cooled (170 K) and then exposed to different amounts of Li indicated by the evaporation times in seconds by the spectra. The lowest spectrum is obtained prior to the additional exposure. The 20 sec of evaporation producing the energy shift from *H* to *M* corresponds to a deposit of around 0.05 ML of Li.

monolayer coverage of Li, and (c) the  $(2 \times 2)$  structure. These spectra give an overview of the valence-band region at a photon energy for which the surface electronic structure of the substrate is particularly pronounced. Spectra (b) and (c) demonstrate that the appearance and disappearance of the 1-ML DQWS (labeled *A*), which is observed with a strong cross section in the near-uv, can be monitored also with soft x rays. The peak labeled *J* is due to the well-known surface state.<sup>13</sup> This state shifts away from  $E_F$  upon Li deposition and disappears before half-monolayer coverage is reached. A small but clear effect of the Li deposition is the appearance of a broad feature labeled *K* in the 1-ML spectrum (b) that is absent in the spectrum for clean Cu (a).

Noteworthy in the Cu  $3d$  band-emission range between 2 and 5.5 eV initial energy is that peak *L* remains intense and at nearly constant energy after Li deposition and structure change. Since this peak has been ascribed to a surface state,<sup>14</sup> one would expect it to be particularly sensitive to the disruption of the substrate surface.

### C. Li on Cu(111)- $2 \times 2$ Li

Upon continued deposition at RT after the  $(2 \times 2)$  structure has formed the DQWS characteristic of this structure (peak *H* in Fig. 8) initially shifts to slightly lower energy and another state appears at around 40 meV (peak *I* in Fig. 8).

If the sample is cooled to 170 K after the transformation to the  $(2 \times 2)$  phase is complete and more Li is then deposited, the spectra change in a different manner. Instead of the gradual downshift observed at RT for the state characteristic of the  $(2 \times 2)$  structure, there is initially, upon Li deposition, a steplike downshift by around 25 meV (peaks *H* and *M* in Fig. 11) showing that even a small Li deposit affects the entire surface. Down to quite small Li doses, around 0.02 ML, the size of the shift is independent of the exact amount of Li added. Upon further depositions new, narrow emission

peaks (*N* and *P* in Fig. 11) come and go indicating that films with well-ordered structure and well-defined thickness are obtained.

## IV. DISCUSSION

### A. Li core-level shifts

The split Li  $1s$  core-level peak observed for the  $(2 \times 2)$  structure (*F* and *G* in Fig. 4) shows that the Li atoms occupy at least two different sites. Some qualitative information regarding the sites can be obtained by comparing the present results with those of previous systematic studies of core-level binding energies for alkali-adsorption systems.<sup>15,16</sup> In cases where the overlayer grows layer by atomic layer the core-level binding energy characteristic of the outermost layer of a 2-ML film is higher than that of the interface layer.<sup>17</sup> During deposition of the second layer one then observes a growing peak on the high-binding-energy side of the peak characteristic of 1 ML. In the present case, the shoulder (*G* in Fig. 4) is on the low-binding-energy side. The sign of this shift relative to the 1-ML peak energy is the same as in a previous study of Na on Al(111) where the additional peak was ascribed to intermixing at the interface.<sup>15</sup> Such an interpretation of the appearance of an extra peak at lower binding energy is in accordance with the general trend that the core-level binding energy is reduced if the coordination of the atom is increased. This trend is exemplified by the shallow *p* states ( $1s$  state in Li) of the alkali metals for which the binding energy characteristic of the surface atoms is generally higher than the binding energy characteristic of the bulk atoms.<sup>18</sup> Another example, particularly interesting in the context of surface intermixing, is the observation that the core-level binding energy for an alkali atom adsorbed on a metal substrate with an open surface structure [such as a (100) surface] is lower than the binding energy for one adsorbed to a more close-packed substrate surface of the same metal [such as a (111) surface].<sup>16</sup>

In the present case, the dominant component (*F* in Fig. 4) of the  $1s$  doublet appears at an energy close to that observed for the adsorbed Li monolayer at full monolayer coverage (*E* in Fig. 4). We therefore associate peak *F* with Li atoms that remain adsorbed and the shoulder (*G*) with Li atoms that occupy substitutional sites. The dominance of one component is in accordance with the LEED result (of Mizuno *et al.*<sup>7</sup>) that there are twice as many adsorbed as substitutional Li atoms in the  $(2 \times 2)$  structure. Also, the small upward binding-energy shift observed for peak *F* relative to peak *E* is as expected for the proposed substitutional structure since the atomic density and thereby coordination of an atom in the overlayer of this structure is somewhat lower than in a close-packed monolayer.

In the submonolayer coverage range, binding-energy downshifts for the adsorbate core levels, such as that observed for Cu(111)/Li (Figs. 5 and 6), as well as excitation threshold downshifts for these levels, are commonly observed upon adsorption of alkali metals on low-index surfaces of metals.<sup>19–24</sup> The origin of binding-energy shifts is in general not easily determined unambiguously, since final-state as well as initial-state contributions must be considered.<sup>22,25,26</sup> However, for Cu(111)/Na it was argued

from the results of a first-principles calculation that a dominant contribution to the binding-energy shift originates in the change of electrostatic potential near the alkali core that results from a coverage-dependent displacement of alkali valence charge towards the substrate.<sup>23</sup> This initial-state effect is likely to make a significant contribution also to the shift observed for the present system.

In previous photoemission work, an abrupt change in Li  $1s$  binding energy with coverage in the submonolayer range was reported for Li deposition on another close-packed metal surface, Be(0001), and this was ascribed to a combined nonmetal-metal and disorder-order transition in the overlayer.<sup>27</sup> In contrast, Cu(111)/Li shows a continuously shifting Li  $1s$  emission peak in the submonolayer coverage range (down to 0.07 ML), without discontinuous changes in line shape or intensity (Figs. 5 and 6). Our results for Cu(111) as a substrate thus indicate a gradual lateral compression of the Li monolayer, accompanied by a smooth increase of its valence-electron density.

### B. Valence states

The downshift for the energy of the monolayer DQWS, as the coverage approaches a full atomic layer, plotted in Fig. 2 for 170 K (although observed also at RT), is ascribed to a more attractive potential as the volume defined by the monolayer is filled with an increasing number of uniformly distributed Li atoms.<sup>5</sup> This interpretation is consistent with the continuous Li  $1s$  binding-energy shift (Figs. 5 and 6) discussed above, which suggests that no Li-island formation occurs in the submonolayer range.

That the energy of the DQWS saturates at  $E_F - 135$  meV when the sample is at 170 K (Fig. 2) and at  $E_F - 110$  meV at RT indicates that the full-monolayer coverage is smaller at RT than at 170 K. From the plot in Fig. 2 of energy versus coverage, one finds that the 25-meV difference corresponds to a 6% smaller saturation coverage at RT. This interpretation is supported by the 25-meV upward shift of the energy observed when, after deposition of a full monolayer at 170 K, the sample is taken to RT. The temperature increase thus leads to a reordering of the atoms at the surface suggesting that the RT threshold for substitution is a few percent smaller than the monolayer saturation coverage at 170 K.

The emission peak  $H$  in Fig. 8, appearing after the transformation into the  $(2 \times 2)$  phase, has the narrow width expected for emission from a DQWS of a well-ordered structure. The long time required to complete the structure change suggests that the reordering involves transport of atoms over long distances and gives loose support to the conclusion from the LEED analysis<sup>7</sup> and the present core-level photoemission data that the observed  $(2 \times 2)$  pattern is due to a structure with Li atoms in substitutional sites and the Cu atoms transferred to expand the terraces. Further support for the suggested structure is obtained from the energy of the DQWS. According to the LEED results,<sup>2</sup>  $\frac{2}{3}$  of the Li atoms remain on top of the mixed outermost layer with Cu atoms. With a total Li coverage of 15% more than required to obtain saturation at RT and a RT saturation coverage that is 6% less than the saturation coverage at low temperature, the top layer coverage in the  $(2 \times 2)$  phase should be 72% of the saturation coverage at low temperature. At this Li coverage on an

undisrupted Cu(111) substrate the DQWS energy obtained from the plot in Fig. 2 is 65 meV. The reduced top-layer coverage resulting from the transformation thus explains a large fraction of the shift from  $-110$  meV for the state characteristic of 1 ML to 100 meV after the structure change. To this shift should be added a shift due to the incorporation of Li atoms in the outermost layer of the substrate. The energy of a DQWS can be estimated from the phase condition  $\Phi_B + \Phi_C + 2\Phi_D = 2\pi m$ , where  $m = 0, 1, 2, \dots$  and the terms on the left-hand side are the phase shifts at the vacuum barrier, the substrate interface, and across the film, respectively.<sup>1,10,11</sup> The 0.3-eV decrease of the work function associated with the structure change is expected to give a slight downshift of the energy. The work function enters the phase condition via  $\Phi_B$ , which depends on energy relative to the vacuum level.<sup>28</sup> In the present case, no estimate of this shift is called for when the energy at 0.72 ML is read off from the plot in Fig. 2 since at that coverage  $e\phi$  has nearly the same value as for the  $(2 \times 2)$  structure. That every fourth Cu atom in the outermost substrate layer is replaced by Li will affect the energy mainly via the phase shift  $\Phi_C$  at the substrate-overlayer interface.  $\Phi_C$  varies from zero to  $\pi$  across the 5-eV-wide energy gap for Cu at the  $L$  point of the Brillouin zone. Substitution of a more free-electron-like metal such as Li is likely to give an effective narrowing of the gap and for states not far from the lower edge of the gap this will lead to an upward energy shift for the DQWS. Of the 210-meV shift observed as the structure transforms, most may thus, we suggest, be explained by a reduced density of Li in the top layer with the remaining part of the shift explained by the incorporation of Li atoms in the substrate.

These findings show that DQWS's can be found in an overlayer above an intermixed interface and that photoemission out of such states can be used as support for the general structure determination methods.

The weak feature  $K$  near 1-eV binding energy in the 1-ML spectrum (b) of Fig. 10 is clearly induced by the Li monolayer since it is absent in the spectrum for clean Cu (a). We propose, however, that it is due to optical  $s, p$ -band transitions in Cu for which the  $k$ -conservation rule at  $h\nu = 70$  eV picks initial states near the low-energy edge  $L_{2'}$  (0.8 eV below  $E_F$ ) of the band gap at the  $L$  symmetry point. The suppression of  $s, p$ -band emission near  $L_{2'}$  for clean Cu(111) [see Fig. 10(a)] has previously been observed by Petroff and Thiry<sup>29</sup> and ascribed to the fact that the density of bulk-band electrons is small close beneath the surface for energies near the band edge. This, as discussed by Inglesfield,<sup>30</sup> is a consequence of the difficulty of fitting a vacuum tail to the standing wave at the zone boundary since the amplitude of this state  $L_{2'}$  has maxima between the (111) planes and thereby a maximum also near the vacuum interface. As a monolayer of Li is deposited on Cu(111), the wave-function boundary condition responsible for the decrease in bulk-band electron density near the surface, for states close to the band edge, is relaxed such that the electron density increases and photoemission from these states may be observed.

For the clean substrate [Fig. 10(a)] the  $s, p$ -band intensity missing at 70 eV is transferred to the surface state, which has an intensity maximum at this photon energy.<sup>14</sup> For the DQWS [Fig. 10(b)] the cross section will get only a small

contribution from the alkali-metal overlayer for photon energies well above the plasmon energy since the film is then transparent. The intensity will therefore be determined by the contribution from the tail of the DQWS in the substrate. This tail is similar to that of the surface state and one thus also expects the DQWS to have a maximum intensity at 70 eV. The main difference between the two states is that for the DQWS the charge is shared between the substrate and the overlayer. Compared to the surface state a smaller fraction of the charge therefore resides in the tail. This explains why the emission intensity relative to the Cu  $3d$  intensity is smaller for the DQWS than for the surface state. Regarding the intensity, one may also note that the DQWS is close to the Fermi energy and has a positive dispersion such that it is observed only for emission angles within around  $2^\circ$  of the surface normal.

### C. Li on Cu(111)- $2\times 2$ Li

The steplike energy shift that occurs when Li is added to the  $(2\times 2)$  structure after cooling the sample to 170 K (see peaks *H* and *M* in Fig. 11) may be explained if the Li deposit is dispersed and each Li atom induces a reordering of the surrounding atoms. Since a deposit of only 0.02 ML is needed for the shift to be observed, the surrounding affected by each Li atom must consist of a large number of atoms.

The behavior thus indicates that the  $(2\times 2)$  structure when cooled to 170 K is unstable with respect to Li adsorption. For this transformation no time delay is noted, which suggests that no long-range transport is necessary. Compared with the 210-meV energy shift of the DQWS, which accompanies the RT transformation to the  $(2\times 2)$  phase, the present 25-meV shift is small and this suggests that the structure change is more modest.

### V. CONCLUSIONS

Our results show that high-resolution photoemission from discrete quantum-well states can be used as a probe of structure changes and growth modes of adsorption systems. In the case of Cu(111)/Li, four different types of atom rearrangements are observed and characterized by the different times required for the reordering and the energies of the characteristic valence-electron states. For one of these rearrangements, namely, that into a  $(2\times 2)$  surface structure, core-level photoemission results are obtained supporting an earlier proposal<sup>7</sup> that it involves the formation of an intermixed Cu-Li atomic layer. Regarding confinement effects, one observation of interest is that discrete quantum-well states may be found in a metal overlayer even when there is intermixing at the interface and that the DQWS energies may be explained semiquantitatively in simple terms.

\*Permanent address: Institute of Physics, National Academy of Sciences of Ukraine, UA-252650 Kiev 28, Ukraine.

<sup>1</sup>S.-Å. Lindgren and L. Walldén, *Solid State Commun.* **34**, 671 (1980); *Phys. Rev. Lett.* **59**, 3003 (1987); **61**, 2894 (1988).

<sup>2</sup>T. Miller, A. Samsavar, and T.-C. Chiang, *Phys. Rev. B* **50**, 17 686 (1994), and references therein.

<sup>3</sup>D. Heskett, K.-M. Frank, E. E. Koch, and H. J. Freund, *Phys. Rev. B* **36**, 1276 (1987).

<sup>4</sup>B. A. McDougall, T. Balasubramanian, and E. Jensen, *Phys. Rev. B* **51**, 13 891 (1995).

<sup>5</sup>A. Carlsson, S.-Å. Lindgren, C. Svensson, and L. Walldén, *Phys. Rev. B* **50**, 8926 (1994).

<sup>6</sup>A. Carlsson, B. Hellsing, S.-Å. Lindgren, and L. Walldén, *Phys. Rev. B* **56**, 1593 (1997).

<sup>7</sup>S. Mizuno, H. Tochihara, A. Barbieri, and M. A. Van Hove, *Phys. Rev. B* **51**, 7981 (1995).

<sup>8</sup>S.-Å. Lindgren, C. Svensson, L. Walldén, A. Carlsson, and E. Wahlström, *Phys. Rev. B* **54**, 10 912 (1996).

<sup>9</sup>I. Lindau and L. Walldén, *Phys. Scr.* **3**, 77 (1971).

<sup>10</sup>A. Beckman, M. Klaua, and K. Meinel, *Phys. Rev. B* **48**, 1844 (1993).

<sup>11</sup>N. V. Smith, N. B. Brookes, Y. Chang, and P. D. Johnson, *Phys. Rev. B* **49**, 332 (1994).

<sup>12</sup>M. Gierer, H. Over, H. Bludau, and G. Ertl, *Phys. Rev. B* **52**, 2927 (1995).

<sup>13</sup>P. O. Gartland and B. J. Slagsvold, *Phys. Rev. B* **12**, 4047 (1975).

<sup>14</sup>S. G. Louie, P. Thirty, R. Pinchaux, Y. Pétrouff, D. Chandresris, and J. Lecante, *Phys. Rev. Lett.* **44**, 549 (1980).

<sup>15</sup>J. N. Andersen, M. Qvarford, R. Nyholm, J. F. van Acker, and E. Lundgren, *Phys. Rev. Lett.* **68**, 94 (1992).

<sup>16</sup>E. Lundgren, M. Qvarford, R. Nyholm, and J. N. Andersen, *Vacuum* **46**, 1159 (1995).

<sup>17</sup>N. Mårtensson, A. Stenborg, O. Björneholm, A. Nilsson, and J. N. Andersen, *Phys. Rev. Lett.* **60**, 1731 (1988); J. N. Andersen, O. Björneholm, A. Stenborg, A. Nilsson, C. Wigren, and N. Mårtensson, *J. Phys.: Condens. Matter* **1**, 7309 (1989); E. Lundgren, J. N. Andersen, M. Qvarford, and R. Nyholm, *Surf. Sci.* **281**, 83 (1993); E. Lundgren, M. Qvarford, R. Nyholm, and J. N. Andersen, *Phys. Rev. B* **50**, 4711 (1994); A. Carlsson, D. Claesson, S.-Å. Lindgren, and L. Walldén (unpublished).

<sup>18</sup>G. K. Wertheim, D. M. Riffe, N. V. Smith, and P. H. Citrin, *Phys. Rev. B* **46**, 1955 (1992).

<sup>19</sup>S.-Å. Lindgren and L. Walldén, *Phys. Rev. B* **22**, 5967 (1980).

<sup>20</sup>G. Pirug, A. Winkler, and H. P. Bonzel, *Surf. Sci.* **163**, 153 (1985).

<sup>21</sup>A. Hohlfeld, M. Sunjić, and K. Horn, *J. Vac. Sci. Technol. A* **5**, 679 (1987).

<sup>22</sup>J. N. Andersen, E. Lundgren, R. Nyholm, and M. Qvarford, *Surf. Sci.* **289**, 307 (1993).

<sup>23</sup>X. Shi, D. Tang, D. Heskett, K.-D. Tsuei, H. Ishida, Y. Morikawa, and K. Terakura, *Phys. Rev. B* **47**, 4014 (1993).

<sup>24</sup>S. Andersson and U. Jostell, *Surf. Sci.* **46**, 625 (1974).

<sup>25</sup>A. R. Williams and N. D. Lang, *Phys. Rev. Lett.* **40**, 954 (1978).

<sup>26</sup>G. A. Benesh and D. A. King, *Chem. Phys. Lett.* **191**, 315 (1992).

<sup>27</sup>G. M. Watson, P. A. Brühwiler, H. J. Sagner, K. H. Frank, and E. W. Plummer, *Phys. Rev. B* **50**, 17 678 (1994).

<sup>28</sup>E. G. McRae and M. L. Kane, *Surf. Sci.* **108**, 435 (1981).

<sup>29</sup>Y. Petroff and P. Thiry, *Appl. Opt.* **19**, 3957 (1980).

<sup>30</sup>J. E. Inglesfield, *Rep. Prog. Phys.* **45**, 223 (1982).